Science of the Total Environment
Manuscript Draft

Manuscript Number: STOTEN-D-18-10789

Title: Application of Air Parcel Residence Time Analysis for Air Pollution Prevention and Control Policy in the Pearl River Delta Region

Article Type: Research Paper

Keywords: Air Parcel Residence Time, Population Exposure to Air Parcel, HYSPLIT, air pollution prevention and control, Pearl River Delta region

Abstract: With the increase in air parcel residence time (APRT) in a certain area, the atmospheric diffusion capacity of the air parcel decreases. Therefore, in this study, the APRT was investigated to study its potential application in air pollution prevention and control in the Pearl River Delta (PRD) region. The APRT in the PRD region was defined as the total period for which an air parcel stays within the PRD region. The Hybrid Single-Particle Lagrangian Integrated Trajectory (HYSPLIT) model was used to calculate the hourly APRT in 2012, 2014, and 2015 based on forward trajectories from 16,720 starting locations. The seasonal APRT results revealed that long APRT was mainly distributed in southern PRD in the summer half year, but in northeastern PRD in the winter half year. This is related to the prevailing wind directions in the summer and winter monsoons. Moreover, the comparison of APRT in different years revealed that the diffusion condition was relatively poor in fall in 2012 and throughout 2014 but was relatively favorable in 2015, which also corresponded to the pollutant concentrations. The APRT calculated from regional air pollution days indicated that the emission reduction strategy should be implemented in the key areas, namely the eastern and central Guangzhou, western Huizou, and the border between Foshan and Jiangmen, and the construction of new factories should not be allowed in these areas. Compared to the APRT, which was investigated to trace the air pollution source, population exposure to air parcels (PEAP) was investigated to orient the influence of path-and-time-weighted sources to population. Consequently, a high PEAP was found to be distributed mainly in the central Guangzhou and Shenzhen and scattered in other urban areas.

*Title Page

Application of Air Parcel Residence Time Analysis for Air Pollution Prevention and Control Policy in the Pearl River Delta Region

Yeqi Huang [a], Teng Yao [a], Jimmy C. H. Fung [a,b*], Xingcheng Lu [a], Alexis K. H. Lau [a,c]

[a] *Division of Environment and Sustainability, The Hong Kong University of Science and Technology, Clear Water Bay, Kowloon, Hong Kong, China*

[b] *Division of Mathematics, The Hong Kong University of Science and Technology, Clear Water Bay, Kowloon, Hong Kong, China*

[c] *Department of Civil and Environmental Engineering, the Hong Kong University of Science and Technology, Hong Kong, China*

Submitted to Science of the Total Environment

*Corresponding author & address: Jimmy C. H. Fung; majfung@ust.hk

*Graphical Abstract

GRAPHICALABSTRACT

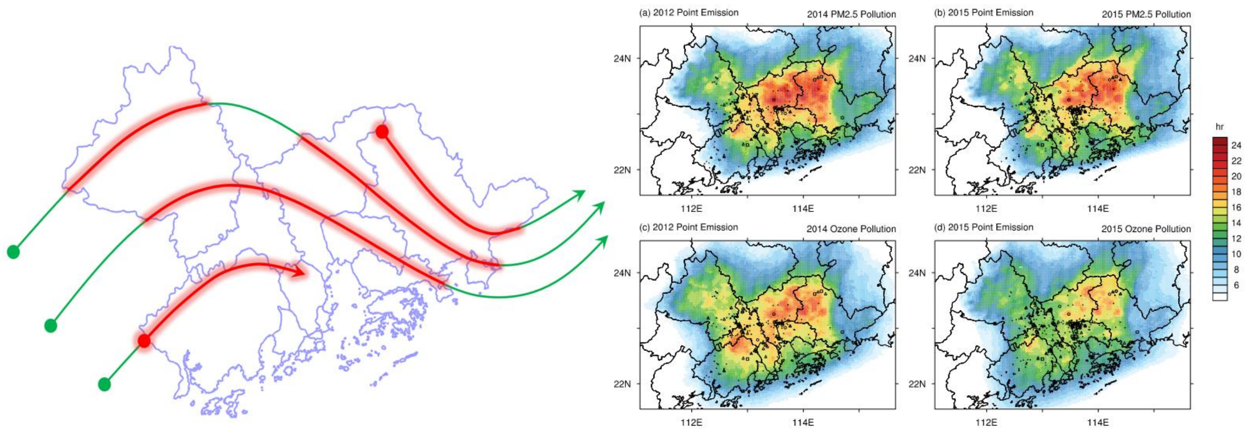

***Highlights (for review : 3 to 5 bullet points (maximum 85 characters including spaces per bullet point)**

HIGHLIGHTS

Air Parcel Residence Time (APRT) was investigated to identify potential emission control regions.

The APRT and traditional emission control methods were compared.

The APRT in the seasonal cycle and on regional air pollution days was analyzed.

Population exposure to air parcels (PEAP) on regional air pollution days was investigated to trace the influence of path-and-time-weighted sources to population.

Application of Air Parcel Residence Time Analysis for Air Pollution Prevention and Control Policy in the Pearl River Delta Region

Yeqi Huang [a], Teng Yao [a], Jimmy C. H. Fung [a,b*], Xingcheng Lu [a], Alexis K. H. Lau [a,c]

[a] *Division of Environment and Sustainability, The Hong Kong University of Science and Technology, Clear Water Bay, Kowloon, Hong Kong, China*

[b] *Division of Mathematics, The Hong Kong University of Science and Technology, Clear Water Bay, Kowloon, Hong Kong, China*

[c] *Department of Civil and Environmental Engineering, the Hong Kong University of Science and Technology, Hong Kong, China*

Submitted to Science of the Total Environment

*Corresponding author & address: Jimmy C. H. Fung; majfung@ust.hk

Abstract

With the increase in air parcel residence time (APRT) in a certain area, the atmospheric diffusion capacity of the air parcel decreases. Therefore, in this study, the APRT was investigated to study its potential application in air pollution prevention and control in the Pearl River Delta (PRD) region. The APRT in the PRD region was defined as the total period for which an air parcel stays within the PRD region. The Hybrid Single-Particle Lagrangian Integrated Trajectory (HYSPLIT) model was used to calculate the hourly APRT in 2012, 2014, and 2015 based on forward trajectories from 16,720 starting locations. The seasonal APRT results revealed that long APRT was mainly distributed in southern PRD in the summer half year, but in northeastern PRD in the winter half year. This is related to the prevailing wind directions in the summer and winter monsoons. Moreover, the comparison of APRT in different years revealed that the diffusion condition was relatively poor in fall in 2012 and throughout 2014 but was relatively favorable in 2015, which also corresponded to the pollutant concentrations. The APRT calculated from regional air pollution days indicated that the emission reduction strategy should be implemented in the key areas, namely the eastern and central Guangzhou, western Huizou, and the border between Foshan and Jiangmen, and the construction of new factories should not be allowed in these areas. Compared to the APRT, which was investigated to trace the air pollution source, population exposure to air parcels (PEAP) was investigated to orient the influence of path-and-time-weighted sources to population. Consequently, a high PEAP was found to be distributed mainly in the central Guangzhou and Shenzhen and scattered in other urban areas.

Keywords: Air Parcel Residence Time, Population Exposure to Air Parcel, HYSPLIT, air pollution prevention and control, Pearl River Delta region

1. Introduction

During the last decade, heavy haze and ozone pollution have occurred frequently in the urban areas of China, especially in the Beijing–Tianjin–Hebei Region, the Yangtze River Delta, and the Pearl River Delta (Li et al., 2014; Zhang et al., 2014; Brauer et al., 2015; He et al., 2017). Exposure to ambient air pollution has been linked to adverse effects on human health and risks of mortality (Delfino et al., 2009; Sicard et al., 2011; Lin et al., 2016). The Chinese government has implemented aggressive strategies to prevent and control further deterioration of air pollution. In September 2013, the State Council of China enacted the "Air Pollution Prevention and Control Action Plan," which contributed to 5.8% and 10.9% reductions in the annual emissions of SO_2 and NO_x, respectively, in 2015. The People's Government of Guangdong Province issued "Guangdong Province Air Pollution Prevention and Control Plan (2014–2017)" in February 2014 with the aim to call on the cooperation of pollution control in the PRD region. Owing to the strict enforcement of these plans, the air quality has continued to improve in the recent years.

The air pollution prevention and control strategies include two important components: emission reduction and emission structure relocation. Recent studies have paid more attention to source and regional contribution diagnoses because they are straightforward and effective methods to guide emission reduction in the current scenario in China. The most common methods used in source and regional contribution diagnoses include the chemical mass balance (CMB) analysis (Yin et al., 2015; Liu et al., 2016; Tang et al., 2018), positive matrix factorization (PMF; Sun et al., 2013; Wang et al., 2015), brute-force method (Wang et al. 2013; Kim et al., 2017; Huang et al., 2018; Deng et al., 2018), particulate matter source apportionment technology, and ozone source apportionment technology (Li et al., 2012; Li et al. 2013; Wang et al., 2014; 2015; Li et al., 2016; Lu, X. and Fung, J.C., 2016a). However, these methods have some limitations in their application for policy making. CMB analysis and PMF can identify potential emission sources only at the fixed observation site, which is insufficient to meet the requirement of the regional emission control strategy. In the case of air quality models, such as the Community Multiscale Air Quality (CMAQ) model and the Comprehensive Air Quality Model with Extensions (CAMx), the uncertainty of emission inventory somewhat diminishes their utility and accuracy. Moreover, it is very time-consuming to simulate emission control scenarios due to the complex calculation in batch of chemical reactions. The subdomains of emission control scenarios should be arranged in advance, and the results should also be limited to the pre-divided subdomains.

The emission structure relocation method is another promising way to control the air pollution, as the emission reduction space in China is relatively restricted at present. However, few studies have focused on this subject. To develop timely recommendations for pollution prevention and control policies, the result should reflect the general situation and the major characteristic of the source contributions. In this study, the concept of air parcel residence time (APRT) was established to identify the regional emission sources. If the same emission reduction strategy is implemented in two regions with different atmospheric diffusion capacity, the contributions of the strategy to the air quality, i.e., its emission control efficiency, would be different in the two regions. Indeed, this emission control efficiency will be better in regions with poor diffusion conditions than in those with favorable diffusion conditions. This concept led to the idea of APRT. Further, the Hybrid Single-Particle Lagrangian Integrated Trajectory (HYSPLIT) model with forward trajectories (Draxler and Hess, 1997, 1998) was used in this study. Without the complex chemistry calculation, the HYSPLIT model can rapidly capture the principal diffusion characteristics and trace the potential emission sources. Previous studies have also used the HYSPLIT model to perform emission control analyses (Makra et al., 2013; Huang et al., 2015; Ni'Am et al., 2017; Yang et al., 2017). For example, Wang et al. (2010) applied this model with a k-means clustering algorithm to classify the transport patterns and indicated that the southwestern transport pathway was associated with the increasing phase of <10-μm particulate matter (PM_{10}). Ding et al. (2017) used backward trajectory and potential source contribution function of the HYSPLIT model to identify the potential source distributions. However, most of the studies set the receptor as a fixed position instead of considering the regional properties because of the limitation of backward trajectory.

Therefore, considering the regional properties, we introduced forward trajectory to calculate the APRT. Sharing the same objective with the previous studies, this study aimed to provide references for policy makers to build the regional air pollution control strategies, considering both source contribution and emission structure relocation. The HYSPLIT configuration and statistical methods are described in Section 2. The results and analysis are presented in Section 3. The summary and discussion are presented in Section 4.

2. Model, data, and analysis methods

2.1 Forward Trajectory of HYSPLIT

The HYSPLIT version 4 updated in February 2016 was used to calculate the 120-h forward trajectories. The HYSPLIT model was driven by meteorological data output from the Weather Research and Forecasting (WRF) model version 3.7.1, which assimilated wind field observation data in the third nested domain. The WRF grid resolutions were 27 km, 9 km, and 3 km, with domain 3 (3 km) covering the entire PRD region with 172 × 130 horizontal grids and 39 vertical layers. In this study, 152 × 110, i.e., 16720, starting locations were chosen to investigate the effect of air parcels from these points, and all air parcels were initiated at each hour in 2012, 2014 and 2015. The starting locations were distributed at every 3 km along the grids within the WRF domain. To investigate the movement of air parcels in the planetary boundary layer, the initial air parcels were released at 100-m height. Two similar experiments were also performed in January 2015 but at 20- and 50-m height. The patterns of the three experiments were quite similar (figure not shown). Therefore, the experiment at 100-m height was selected as the representative in this study.

2.2 APRT

In total, 16,720 air parcels were uniformly released at 100-m height from the starting locations, and the total period for which an air parcel stayed within the PRD region was defined as the APRT. For example, as the four forward trajectories shown in Fig. 1, no matter where the starting locations were (within or out of the PRD region) or how the trajectories passed through the PRD region (pass directly or go back and forth), the APRT was defined as the total period for which each trajectory stayed in the PRD region (bold red streamlines in Fig. 1). A shorter transport time is associated with a higher wind speed and better atmospheric diffusion capacity, indicating the dilution of air pollutants. By contrast, a long residence time of an air parcel in a certain area (the PRD region in this study) indicates a lower wind speed and poor atmospheric diffusion capacity. Therefore, compared with the regions with short APRT, those with longer APRT can be associated with higher contribution to air pollution in the PRD region. Thus, the spatial gridded APRT can be obtained to identify the potential air pollution prevention and control areas.

2.3 $PM_{2.5}$ and O_3 regional pollution days

The hourly $PM_{2.5}$ and O_3 concentrations in 2014 and 2015 declared by China National Environmental Monitoring Center and Hong Kong Environmental Protection Department were used to indicate the air pollution situation in the PRD region. Because the nationwide regulatory air quality monitoring network was not paved until the end of 2012, the data of 2012 were not considered in this study. The data of 79 (83) stations involving 5 Hong Kong stations in 2014 (2015) were chosen to calculate the daily mean $PM_{2.5}$ and O_3 concentrations. The calculation of daily mean eliminated the missing data in strict accordance with the "Ambient Air Quality Standards of the PRC" (MEP & AQSIQ, 2012).

A $PM_{2.5}$ regional pollution day was defined as a daily $PM_{2.5}$ concentration of >75 μg/m^3 in >10% stations (the second $PM_{2.5}$ standard of "Ambient Air Quality Standards of the PRC"). Similarly, an ozone regional pollution day was defined as a maximum daily mean 8-h ozone concentration of >160 μg/m^3 in >10% stations.

2.4 Population Exposure to Air Parcel (PEAP)

PEAP was defined as the integration of population density along the trajectory. Namely, along the trajectory, the population density and APRT in a certain grid are the functions of time t; thus,

$$\mathrm{PEAP} = \int_L de(s) = \int_{ts}^{te} p(t)dt$$

where L is the trajectory, e(s) is the population exposure on a short section of the trajectory, p is the population density, ts is the start time of the air parcel trajectory, and te is the end time.

The 3 × 3-km population density from High Resolution Global Population Data Set developed by Oak Ridge National Laboratory (Bright et al., 2014) was used in this study, and its distribution is shown in Fig. 2. The figure shows that most of the population in the PRD region is concentrated in the urban areas, especially in Guangzhou, Foshan, Dongguan, and Shenzhen, which are highly urbanized. Over a certain site, the effect of an air parcel on population is determined by the product of local population density and the APRT. For example, if an air parcel has a long APRT and passes through highly populated regions, it will highly affect the population. By contrast, if the trajectory passes through the regions with low population density, a long APRT can have a potentially high contribution to air pollution but little effect on the population.

3. Results

3.1 Seasonal cycle of APRT

Louie et al. (2005) determined seasons that were more applicable to the PRD region, which is located in the Asian monsoon region. Accordingly, in this study, we defined a prolonged summer (May 16 to September 15), winter (January 1 to March 15 and November 16 to December 31), brief spring (March 16 to May 15), and fall (September 16 to November 15). The seasonal cycle of APRT in 2012, 2014, and 2015 and the 200-m terrain height are shown in Fig. 3 to help identify the potential air pollution prevention and control regions. The distribution patterns of the APRT in the same season in different years were quite similar, implying the yearly periodic variations in meteorological conditions, i.e., the patterns of the four seasons show obvious seasonal characteristics related to the summer and winter monsoons. In the summer half year, southerly and southeasterly winds with moderate wind speed predominate in the PRD region. Therefore, air parcels in the southern PRD region travel long time within the PRD region (Fig. 3a-b, e-f, and i-j). The APRT is long in Zhuhai, central Jiangmen, Zhongshan, Shenzhen, Hongkong, the southern Dongguan, and the border between Shenzhen and Huizhou in spring. Meanwhile, in summer, the APRT pattern expands more to the north including the central and southern Zhaoqing and southern Guangzhou. By contrast, during the northeasterly controlled winter half year, air parcels with long residence time are concentrated mainly in the northeastern part of the PRD region (Fig. 3c-d, g-h, and k-l), especially in northeastern and central

Guangzhou, western Huizhou, northern Dongguan, and the border between Foshan and Jiangmen. A relatively long APRT is also distributed in the mountainous regions and along the coastline because the APRT patterns are affected by land–sea breeze circulation and mountain–valley breeze circulation. After the sunset, the updraft of sea breeze circulation returns ashore and results in a longer APRT along the coastline. At the same time, the updraft of mountain–valley breeze circulation moves to the valley, leading to a patchy APRT pattern over the mountainous regions. Due to the relatively low atmospheric diffusion capacity in the nighttime, the mean APRT in the nighttime is longer than that in the daytime. Therefore, the APRT around the coastline and mountainous regions is longer, indicating a greater effect on air quality in the nighttime. This phenomenon can be observed in the diurnal circle of APRT (figure not shown). In the winter half year, the PRD region is dominated by the cold front and high-pressure ridge with a deep thermal inversion layer. Low wind speed and low planetary boundary height in that situation contribute to the low atmospheric diffusion capacity. Therefore, the mean APRT in fall is much longer than that in the summer half year. However, the mean APRT in winter is relatively shorter because some cold air surge with high wind speed decreases the mean wintertime APRT.

The spatial distribution patterns among the APRT of 2012, 2014, and 2015 are similar, while the magnitudes are quite different.. The comparison of the APRT distribution patterns in the same seasons in 2012, 2014 and 2015 clearly showed that the APRT in 2014 was much longer than that in 2012 (except fall) and 2015 (Fig. 3). This feature represents relatively adverse dispersion situations in 2012 fall and throughout 2014, whereas a favorable atmospheric diffusion capacity in 2015.

To learn more about the relation between the regional air pollution and the APRT, we calculated the regional maxima of the APRT, seasonal mean of the APRT, and regional means of $PM_{2.5}$ and O_3 concentrations (see Table 1). The regional mean of the APRT was calculated after removing the values lower than 5 h, which have little effect on the PRD air pollution. During the same season in different years, the maximum and mean APRTs corresponded to the pollutant concentrations, i.e., a long APRT was always accompanied with severe regional air pollution. In general, unfavorable diffusion condition leads to not only the increase in $PM_{2.5}$ and O_3 concentrations but also the accumulation of their precursors. However, the variations in pollutant concentrations were not accompanied by changes in the APRT in different seasons of the same year because the magnitude and direction of horizontal transport, vertical diffusion capacity, and chemical reaction rate were significantly distinct in different seasons. As shown in Table 1, the maximum and mean APRTs in spring 2014 were 19.2 and 10.1 h and 2.2 and 0.8 h longer than those in 2012 and 2.9 and 1.2 h longer than those in 2015, respectively. The regional mean $PM_{2.5}$ concentration in 2014 was 40.5 μg/m^3, which was much larger than 29.4 μg/m^3 in 2015. However, the O_3 concentration in 2014 was a little lower than that in 2015 which may be related to the chemical reaction. In summer, the maximum and mean APRTs in 2014 were 20.0 and 10.7 h and 1.8 and 0.9 h longer than those in 2012 and 3.6 and 1.3 h longer than those in 2015, respectively. When the wind direction became southerly, clean air from the sea decreased the $PM_{2.5}$ concentration. At the same time, as temperature increased, the regional mean O_3 concentration increased to 84.0 and 76.6 μg/m^3 in 2014 and 2015, respectively. In a similar meteorological condition, the favorable diffusion condition in 2015 led to an air quality superior to that in 2014. The longest APRT in fall occurred in 2012, with the maximum value reaching 24.1 h, indicating that some air parcels in the PRD region stayed for >1 day. The longest APRT in fall 2012 was 1.7 h longer than the longest APRT in fall 2014. However, their mean APRT values were close to each other, indicating that areas with long APRT were more concentrated in 2012 than that in 2014 (Fig. 3c and g). The maximum and mean APRTs in fall 2015 were shorter than those in the other seasons of 2012 and 2014. The difference between the air pollutant concentrations in 2014 and 2015 can also explain the severe air pollution in 2014. The APRTs in winter were not significantly different between the 3 years: the maximum values were 17.4, 17.9, and 17.0 h and the mean values were 8.9, 9.2, and 9.0 h in 2012, 2014, and 2015, respectively. One main reason may be that the cold air surge with high wind speed predominantly affected the overall APRT. As shown in Fig. 3h and l, the locations with long APRT in 2014 were more scattered than those in 2015, which may have led to the more severe air pollution in 2014. Although we did not have sufficient air pollution data of 2012, the information in some other reports and studies supported our conclusion. For example, according to the Report on the State of Guangdong Provincial Environment, the annual mean $PM_{2.5}$ concentration in 2011, 2012, 2013, 2014, and 2015 were 54, 50, 60, 60, and 51 $\mu g/m^3$, respectively, demonstrating the rapid improvement in air quality in 2012. Such a phenomenon was also observed by Lin et al. (2016) in the annual mean satellite-retrieved $PM_{2.5}$ concentration. Therefore, the improvement in air quality in 2012 and 2015 may be attributable to not only the emission reduction policies but also better atmospheric diffusion capacities.

3.2 Features of APRT on regional air pollution days

In actual application, policy makers are mostly concerned about the emission control on air pollution days. In response to the inter-regional air pollution prevention and control policy, we calculated the mean APRTs on regional pollution days to assess the pollutant dispersion condition. As the observation data of 2012 were insufficient to reflect the regional pollution, we considered the pollutant dispersion conditions of only 2014 and 2015. Figure 4 shows the mean

APRT on pollution days, and the locations of point emissions in 2012 and 2015 were overlapped onto the APRT maps of 2014 and 2015, respectively. The change in the emission locations served as the reference in the transformation of point emissions. Different levels of emission loads were indicated by a series of markers to assess the tangible effect of the air parcel from the locations. Point sources were found to contribute a large percentage of pollutant emissions, such as SO_2 (>90%), NO_x (>50%), and $PM_{2.5}$ and PM_{10} (>30%), which were also easy to be managed and controlled.

According to the calculation method in Sec. 2.3, 74 $PM_{2.5}$ and 92 O_3 regional pollution days were selected in 2014, and 50 $PM_{2.5}$ and 109 O_3 regional pollution days were selected in 2015. The $PM_{2.5}$ regional pollution days mainly occurred in fall and winter, and O_3 regional pollution days mostly occurred in summer and fall. Therefore, the APRT pattern during $PM_{2.5}$ regional pollution days was similar to that during the winter half year (Fig 4a-b). The APRT pattern during O_3 regional pollution days was also similar to that in the winter half year (Fig 4c-d) because the APRT was longer in fall than in summer. Most studies had set the pre-divided areas according to administrative divisions. However, as shown in Fig. 4, the potential sources are not distributed as per the administrative divisions but as the natural property of the air trajectories with irregular shapes; such a distribution performs better than that based on the administrative divisions. For example, Wu et al. (2013) divided 11 source regions and Li et al. (2012) divided 12 source regions as administrative divisions within and around the PRD region and used the source apportionment technology in CAMx to identify the potential emission control sources. Both groups found a high contribution of non-local emissions to ambient pollutants. However, only part of the potential sources they found were the main contributors. Thus, such a pre-divided method leads to some extra considerations regarding the main contributing regions and some overlooks in other regions. Moreover, it is difficult to make cross-regional pollution control policies, as the contributions are relatively independent.

The similarity of the APRT patterns in different years and pollution situations makes long-term policy making convenient. As mentioned above, the grids with warmer colors represent longer APRTs, indicating the key areas in which to implement the air pollution prevention and control policy. Therefore, the main control areas on regional pollution days include eastern and central Guangzhou, especially Zengcheng, eastern Conghua, Luogang, and eastern Baiyun districts; western Huizhou, such as Longmen, Boluo, and western Huicheng districts; and the border between Foshan and Jiangmen, including the southern Gaoming and Heshan districts. Notably, most of the high emission locations and the potential source regions did not overlap, mostly because most of the potential source regions were mountainous regions, where the air parcels are easily trapped. However, some point emissions were located in severe potential areas (red color codes), such as the central Guangzhou and northern Huizhou, whereas most point emissions occurred in mild potential areas (orange and yellow color codes). If the emission control policy is implemented in the PRD region, these point emissions should be prioritized. Notably, when the diffusion condition is relatively favorable, the air parcels with high residence time mainly come from the mountainous regions with few anthropogenic sources (Fig. 4d). However, when the atmospheric diffusion capacity decreases, the long APRT areas extend to the manufacturing districts (Fig. 4b) and even urban regions with large mobile and resident emissions (Fig. 4a and c). Therefore, the effect of the emissions may increase rapidly when the meteorological situation worsens, which also explains why the regional air pollution occurs within a short time in an adverse dispersion situation.

Emission relocation is another important task in the pollution prevention and control policy of China. In “the Atmospheric Pollution Prevention and Control Law of the People’s Republic of China” (Committee of the NPC, 2015), one approach to prevent and control air pollution is “optimizing industrial structure and distribution and adjusting energy structures.” The policy “Vacating the Cage and Change Birds” (in Chinese Teng Long Huan Niao) proposed by the Guangdong government to relocate traditional manufacturing from PRD to the western and eastern Guangdong province has been thought to have improved the air quality in the PRD region (Yang C., 2012; Yin et al., 2017). In addition, new construction of industries is always considered in future development. The policy makers proposed that “when planning industrial parks, development zones and regional industrial development are likely to increase air pollution in the key regions” (Committee of the NPC, 2015), indicating the importance of location selection for new factories. Based on the conclusion of this study, the relocation or new construction of emission sources from 2012 to 2015 (Fig. 4a–d) led to some improvements and some unfavorable changes in the air quality of PRD as some emission sources have been moved to areas with short APRTs, whereas others have been moved to areas with long APRTs. For example, the increase in emission sources built in Zhaoqing, Jiangmen, central and southern Foshan, Shenzhen, central Dongguan, and eastern Huizhou will decrease air pollution in the PRD region compared with sources built in other areas with longer APRTs, whereas the new settlement on the border between Foshan and Guangzhou, the border between Zhongshan and Guangzhou, northern Guangzhou, northern and central Huizhou, and western Dongguan will deteriorate the air quality of the PRD region because the APRTs in these areas are long. Notably, the local air quality is always most affected by the local emissions. Therefore, in this study, we defined the contribution of an emission location as its total effect on the air quality of the entire PRD region and not on the local air quality alone. The guiding significance of this study was an emission control strategy based on a comprehensive outlook instead of regional consideration alone as reported in traditional studies.

3.3 Features of PEAP on regional air pollution days

One of the most important aims of air pollution prevention and control is to protect population health. As described by World Health Organization (2016), "outdoor air pollution is a major environmental health problem affecting everyone in developed and developing countries alike," and population exposure assessment has been a topic of interest in air pollution studies. Because an overview of control regions is required for policy making, evaluation of the population exposure should be preferred over that of the individual health burden. "Atmospheric Pollution Prevention and Control Law of the People's Republic of China" (2015) proposes the following: "take necessary steps to manage public health risks, according to the air pollutant's potential damage and impact on human health and the environment." One of the traditional methods to estimate spatial population exposure is to calculate the product of spatial distribution of ambient pollutant concentrations and population density (Hystad et al., 2011; Lin et al., 2016; Lu et al., 2016b). Studies that used this method could reveal the health burden caused by the ambient pollutants but could not identify the potential emission control regions.

Based on the concept of APRT and its features on air pollution days stated above, we further investigated PEAP to identify the potential pollution control areas for population on regional pollution days. According to the definition in Sec. 2.4, the concept of PEAP is different from that of traditional population exposure. PEAP can identify the potential influential sources instead of the simple population exposure to the ambient air pollution.

The peak of PEAP was mainly distributed in the central and urban areas of Guangzhou and central Shenzhen and was scattered in the urban areas of other cities. As displayed in Fig. 5, the population density strongly affects the APRT distribution, although PEAP is the product of APRT and population density. Therefore, PEAP basically follows the population density distribution in the PRD region. PEAP is sensitive to the air parcel's starting location; if the starting location is present in a highly populated region, the air parcel has higher probability to affect more population. The warmer colors indicate where the air parcel will affect more population in its trajectory life. The Luogang district and urban Guangzhou were the regions with the greatest effect on the PRD region because of a long APRT and a high population density, respectively. Limited point emissions were found in Guangzhou; however, a few large emissions were located in the high PEAP regions, likely to affect large population in the PRD region. The APRT in Shenzhen and Hong Kong was short (Fig. 4), but the high population density in these regions led to the second highest PEAP. Dongguan and Foshan urban areas have both large population and long APRT; therefore, high PEAP values were also concentrated in these regions. Meanwhile, many high point emissions were located in Dongguan, especially on the border between Dongguan and Guangzhou. These point emissions require attention because they may considerably affect the population health. By contrast, although many point emissions were located in Foshan, they were in areas with low PEAP. Notably, the urban areas mentioned above harbor large mobile and resident emissions, which may cause greater effects than point emissions. Although western Huizhou had long APRT, the high PEAP was limited to the highly populated region and the border between Dongguan and Shenzhen. In addition, the high PEAP in Zhuhai, Jiangmen, and Zhongshan were due to high population density, whereas air parcels from Zhaoqing had little effect on the population of the PRD region.

4. Summary and Discussion

A series of air pollution prevention and control policies have been issued by the government to deal with severe air pollution in the PRD region. However, the precise sources of air pollution in this region remain unknown. In this study, the hourly forward trajectories from 16,720 starting locations were applied to calculate the gridded APRT in 2012, 2014, and 2015. The seasonal cycle of the APRT distribution patterns were found to be related to the summer and winter monsoon, as the long APRT was distributed mainly in southern PRD in the summer half year, whereas in northeastern PRD in the winter half year. The mean APRT in fall was longer than that in the summer half year as the poor atmospheric diffusion condition in fall favors heavy air pollution. However, the APRT in winter was shorter because cold surge with very high wind speed decreased the mean wintertime APRT. The APRT was short in 2015, indicating the favorable diffusion condition, which corresponded to the low $PM_{2.5}$ and O_3 concentrations. By contrast, the long APRT in fall 2012 and throughout 2014 implies the unfavorable atmospheric diffusion capacity and severe air pollution. The APRT patterns on regional air pollution days revealed the potential emission control regions, including eastern and central Guangzhou, western Huizhou, and the border between Foshan and Jiangmen. PEAP on regional air pollution days was investigated to orient the potential influential sources on population. Emission control areas associated with a high PEAP were mainly distributed in the central and urban areas of Guangzhou and central Shenzhen. According to the PEAP pattern, mobile and resident emissions in urban areas may have contributed more than point emissions to population.

The application of APRT can effectively solve some problems in the diagnosis of regional air pollution contribution. The potential sources identified by the APRT and PEAP were not distributed by artificial segregation such as administrative divisions but by the natural property of air trajectories. In addition, the emission inventory keeps changing, but APRT estimation does not require emission inventory and can clearly distinguish the meteorological influence from the total contribution. Moreover, the research object in this study was set as the PRD region to reflect the requirement of inter-regional cooperation in air pollution prevention and control policies. Therefore, the APRT is a simple and suitable concept for providing suggestions and rapid responses as well as for long-term policy making. The APRT analysis can not only be used in emission source orientation but also be applied in emission structure relocation, which is a potential main task in the future. However, the APRT analysis has several limitations because it is a simple concept that lacks the consideration of chemical reactions/pollutants. On the one hand, the lack of chemical reaction calculation may cause inaccuracies when the formation of secondary pollutants predominates. This drawback is reflected in the nonconformity between APRT and O_3 concentration. On the other hand, the weight of the trajectory transport distance may also be an important factor that may have led to some underestimation in the beginning period and overestimation in the ending period of the trajectory life. Nevertheless, the concept of APRT could present an overall picture of potential emission control regions and compensate for some deficiencies in the traditional emission control methods to a certain extent. It is promising tool for application in the making of future prevention and control policies in the PRD region, especially after the two abovementioned limitations are managed.

Acknowledgement

We appreciate the assistance of the Hong Kong Observatory (HKO), which provided the meteorological data. This work was supported by the MOST grant 2018YFC0213903, NSFC Grant 41575106 and RGC Grant 16300715.

REFERENCES

Brauer, M., Freedman, G., Frostad, J., Van Donkelaar, A., Martin, R.V., Dentener, F., Dingenen, R.V., Estep, K., Amini, H., Apte, J.S. and Balakrishnan, K., 2015. Ambient air pollution exposure estimation for the global burden of disease 2013. *Environmental science & technology*, *50*(1), pp.79-88.

Bright, E.A., Coleman, P.R., Rose, A.N. and Urban, M.L., 2014. Landscan. *Oak Ridge: Oak Ridge National Laboratory*.

Chinese State Council, 2013. Atmospheric Pollution Prevention and Control Action Plan (in Chinese). (available online at: http://www.gov.cn/zwgk/2013-09/12/content_2486773.htm).

Delfino, R.J., Staimer, N., Tjoa, T., Gillen, D.L., Polidori, A., Arhami, M., Kleinman, M.T., Vaziri, N.D., Longhurst, J. and Sioutas, C., 2009. Air pollution exposures and circulating biomarkers of effect in a susceptible population: clues to potential causal component mixtures and mechanisms. *Environmental health perspectives*, *117*(8), p.1232.

Deng, T., Huang, Y., Li, Z., Wang, N., Wang, S., Zou, Y., Yin, C. and Fan, S., 2018. Numerical simulations for the sources apportionment and control strategies of $PM_{2.5}$ over Pearl River Delta, China, part II: Vertical distribution and emission reduction strategies. *The Science of the total environment*. 634, pp.1645-1656.

Department of Environmental Protection of Guangdong Province, Report on the State of Guangdong Provincial Environment (in Chinese). (available online at: http://www.gdep.gov.cn/hjjce/gb/)

Ding, X., Kong, L., Du, C., Zhanzakova, A., Wang, L., Fu, H., Chen, J., Yang, X. and Cheng, T., 2017. Long-range and regional transported size-resolved atmospheric aerosols during summertime in urban Shanghai. *Science of the Total Environment*, *583*, pp.334-343.

Draxler, R.R. and Hess, G.D., 1997. Description of the HYSPLIT4 modeling system.

Draxler, R.R. and Hess, G.D., 1998. An overview of the HYSPLIT_4 modelling system for trajectories. *Australian meteorological magazine*, *47*(4), pp.295-308.

He, J., Gong, S., Yu, Y., Yu, L., Wu, L., Mao, H., Song, C., Zhao, S., Liu, H., Li, X. and Li, R., 2017. Air pollution characteristics and their relation to meteorological conditions during 2014–2015 in major Chinese cities. *Environmental pollution*, *223*, pp.484-496.

Huang, Z., Huang, J., Hayasaka, T., Wang, S., Zhou, T. and Jin, H., 2015. Short-cut transport path for Asian dust directly to the Arctic: a case study. *Environmental Research Letters*, *10*(11), p.114018.

Huang, Y., Deng, T., Li, Z., Wang, N., Yin, C., Wang, S. and Fan, S., 2018. Numerical simulations for the sources apportionment and control strategies of $PM_{2.5}$ over Pearl River Delta, China, part I: Inventory and $PM_{2.5}$ sources apportionment. *The Science of the total environment*. 634, pp.1631-1644.

Hystad, P., Setton, E., Cervantes, A., Poplawski, K., Deschenes, S., Brauer, M., van Donkelaar, A., Lamsal, L., Martin, R., Jerrett, M. and Demers, P., 2011. Creating national air pollution models for population exposure assessment in Canada. *Environmental health perspectives*, *119*(8), p.1123.

Kim, H.C., Kim, E., Bae, C., Cho, J.H., Kim, B.U. and Kim, S., 2017. Regional contributions to particulate matter concentration in the Seoul metropolitan area, South Korea: seasonal variation and sensitivity to meteorology and emissions inventory. *Atmospheric Chemistry and Physics*, *17*(17), pp.10315-10332.

Li, J., Lu, K., Lv, W., Li, J., Zhong, L., Ou, Y., Chen, D., Huang, X. and Zhang, Y., 2014. Fast increasing of surface ozone concentrations in Pearl River Delta characterized by a regional air quality monitoring network during 2006–2011. *Journal of Environmental Sciences*, *26*(1), pp.23-36.

Li, L., An, J.Y., Shi, Y.Y., Zhou, M., Yan, R.S., Huang, C., Wang, H.L., Lou, S.R., Wang, Q., Lu,

Q. and Wu, J., 2016. Source apportionment of surface ozone in the Yangtze River Delta, China in the summer of 2013. *Atmospheric Environment*, *144*, pp.194-207.

Li, L., Cheng, S., Li, J., Lang, J. and Chen, D., 2013. Application of MM5-CAMx-PSAT Modeling Approach for Investigatings Emission Source Contribution to Atmospheric Pollution in Tangshan, Northern China. *Mathematical Problems in Engineering*, *2013*.

Li, Y., Lau, A.H., Fung, J.H., Zheng, J.Y., Zhong, L.J. and Louie, P.K.K., 2012. Ozone source apportionment (OSAT) to differentiate local regional and super- regional source contributions in the Pearl River Delta region, China. *Journal of Geophysical Research: Atmospheres*, *117*(D15).

Lin, C., Li, Y., Lau, A.K., Deng, X., Tim, K.T., Fung, J.C., Li, C., Li, Z., Lu, X., Zhang, X. and Yu, Q., 2016. Estimation of long-term population exposure to $PM_{2.5}$ for dense urban areas using 1-km MODIS data. *Remote sensing of environment*, *179*, pp.13-22.

Liu, Q., Baumgartner, J., Zhang, Y. and Schauer, J.J., 2016. Source apportionment of Beijing air pollution during a severe winter haze event and associated pro-inflammatory responses in lung epithelial cells. *Atmospheric Environment*, *126*, pp.28-35.

Louie, P.K., Watson, J.G., Chow, J.C., Chen, A., Sin, D.W. and Lau, A.K., 2005. Seasonal characteristics and regional transport of $PM_{2.5}$ in Hong Kong. *Atmospheric Environment*, *39*(9), pp.1695-1710.

Lu, X. and Fung, J.C., 2016a. Source Apportionment of Sulfate and Nitrate over the Pearl River Delta Region in China. *Atmosphere*, *7*(8), p.98.

Lu, X., Yao, T., Li, Y., Fung, J.C. and Lau, A.K., 2016b. Source apportionment and health effect of NO_x over the Pearl River Delta region in southern China. *Environmental pollution*, *212*, pp.135-146.

Makra, L., Ionel, I., Csépe, Z., Matyasovszky, I., Lontis, N., Popescu, F. and Sümeghy, Z., 2013. The effect of different transport modes on urban PM_{10} levels in two European cities. *Science of the Total Environment*, *458*, pp.36-46.

Ministry of Environmental Protection and State Administration for Quality Supervision and Inspection and Quarantine, 2012. Ambient Air Quality Standards of the PRC (in Chinese). (available online at: http://210.72.1.216:8080/gzaqi/Document/gjzlbz.pdf)

Ni'Am, M., Sitanggang, I.S. and Nuryanto, D.E., 2017, January. Clustering of CO and CO_2 concentration from Sumatra peat fire haze using HYSPLIT and K-means algorithm. In *IOP Conference Series: Earth and Environmental Science* (Vol. 54, No. 1, p. 012054). IOP Publishing.

People's government of Guangdong Province, 2014. Guangdong Province Air Pollution Prevention and Control Plan (2014-2017) (in Chinese). (available online at: http://www.gdep.gov.cn/zcfg/dfguizhang/201703/t20170307_220796.html)

Sicard, P., Lesne, O., Alexandre, N., Mangin, A. and Collomp, R., 2011. Air quality trends and potential health effects–development of an aggregate risk index. *Atmospheric Environment*, *45*(5), pp.1145-1153.

Standing Committee of the National People's Congress, 2015. Atmospheric Pollution Prevention and Control Law of the People's Republic of China (2015 Revision) (in Chinese). (available online at: http://www.npc.gov.cn/npc/xinwen/2015-08/31/content_1945589.htm)

Sun, Y.L., Wang, Z.F., Fu, P.Q., Yang, T., Jiang, Q., Dong, H.B., Li, J. and Jia, J.J., 2013. Aerosol composition, sources and processes during wintertime in Beijing, China. *Atmospheric Chemistry and Physics*, *13*(9), pp.4577-4592.

Tang, R., Wu, Z., Li, X., Wang, Y., Shang, D., Xiao, Y., Li, M., Zeng, L., Wu, Z., Hallquist, M.

and Hu, M., 2018. Primary and secondary organic aerosols in summer 2016 in Beijing. *Atmospheric Chemistry and Physics*, *18*(6), pp.4055-4068.

Wang, F., Chen, D.S., Cheng, S.Y., Li, J.B., Li, M.J. and Ren, Z.H., 2010. Identification of regional atmospheric PM_{10} transport pathways using HYSPLIT, MM5-CMAQ and synoptic pressure pattern analysis. *Environmental Modelling & Software*, *25*(8), pp.927-934.

Wang, L.T., Wei, Z., Yang, J., Zhang, Y., Zhang, F.F., Su, J., Meng, C.C. and Zhang, Q., 2013. The 2013 severe haze over the southern Hebei, China: model evaluation, source apportionment, and policy implications. *Atmospheric Chemistry & Physics Discussions*, *13*(11).

Wang, Q., Sun, Y., Jiang, Q., Du, W., Sun, C., Fu, P. and Wang, Z., 2015. Chemical composition of aerosol particles and light extinction apportionment before and during the heating season in Beijing, China. *Journal of Geophysical Research: Atmospheres*, *120*(24), pp.12708-12722.

Wang, Y., Li, L., Chen, C., Huang, C., Huang, H., Feng, J., Wang, S., Wang, H., Zhang, G., Zhou, M. and Cheng, P., 2014. Source apportionment of fine particulate matter during autumn haze episodes in Shanghai, China. *Journal of Geophysical Research: Atmospheres*, *119*(4), pp.1903-1914.

World Health Organization (WHO), 2016. Ambient (outdoor) air quality and health. (available online at: http://www.who.int/mediacentre/factsheets/fs313/en/)

Wu, D., Fung, J.C.H., Yao, T. and Lau, A.K.H., 2013. A study of control policy in the Pearl River Delta region by using the particulate matter source apportionment method. *Atmospheric Environment*, *76*, pp.147-161.

Yang, C., 2012. Restructuring the export-oriented industrialization in the Pearl River Delta, China: Institutional evolution and emerging tension. *Applied Geography*, *32*(1), pp.143-157.

Yang, W., Wang, G. and Bi, C., 2017. Analysis of Long-Range Transport Effects on $PM_{2.5}$ during a Short Severe Haze in Beijing, China. *Aerosol and Air Quality Research*, *17*, pp.1610-1622.

Yin, J., Cumberland, S.A., Harrison, R.M., Allan, J., Young, D.E., Williams, P.I. and Coe, H., 2015. Receptor modelling of fine particles in southern England using CMB including comparison with AMS-PMF factors. *Atmospheric Chemistry and Physics*, *15*(4), pp.2139-2158.

Yin, X., Huang, Z., Zheng, J., Yuan, Z., Zhu, W., Huang, X. and Chen, D., 2017. Source contributions to $PM_{2.5}$ in Guangdong province, China by numerical modeling: Results and implications. *Atmospheric Research*, *186*, pp.63-71.

Zhang, Q., Yuan, B., Shao, M., Wang, X., Lu, S., Lu, K., Wang, M., Chen, L., Chang, C.C. and Liu, S.C., 2014. Variations of ground-level O_3 and its precursors in Beijing in summertime between 2005 and 2011. *Atmospheric Chemistry and Physics*, *14*(12), pp.6089-6101.

Tables and Figures

Table 1 Seasonal maximum APRT, seasonal mean APRT, $PM_{2.5}$ concentration, and O_3 concentration in 2012, 2014, and 2015

Seasons	Variables	2012	2014	2015
Spring	APRT_MAX (h)	17.0	19.2	16.3
	APRT_AVG (h)	9.3	10.1	8.9
	$PM_{2.5}$ (μg/m^3)	/	40.5	29.4
	O_3 (μg/m^3)	/	70.4	71.7
Summer	APRT_MAX (h)	18.2	20.0	16.4
	APRT_AVG (h)	9.6	10.7	9.4
	$PM_{2.5}$ (μg/m^3)	/	24.8	23.9
	O_3 (μg/m^3)	/	84.0	76.6
Fall	APRT_MAX (h)	24.1	22.4	19.2
	APRT_AVG (h)	11.3	11.0	9.8
	$PM_{2.5}$ (μg/m^3)	/	47.6	38.4
	O_3 (μg/m^3)	/	103.3	85.6
Winter	APRT_MAX (h)	17.4	17.9	17.0
	APRT_AVG (h)	8.9	9.2	9.0
	$PM_{2.5}$ (μg/m^3)	/	55	43.2
	O_3 (μg/m^3)	/	66.0	55.2

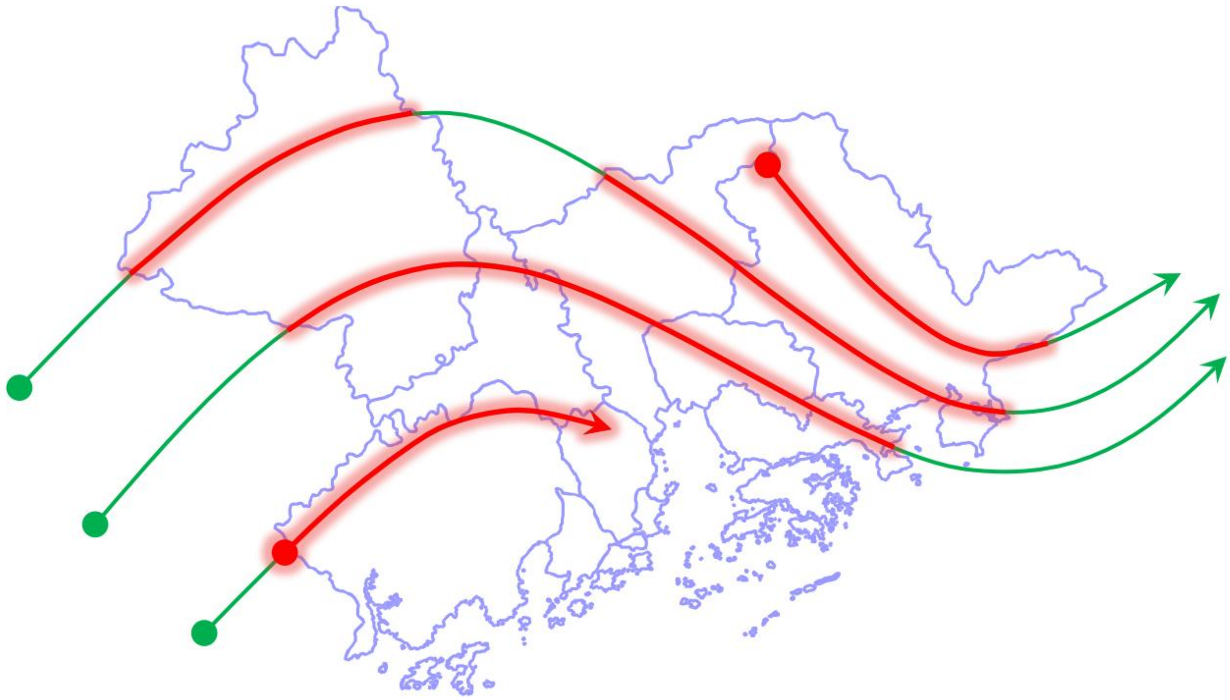

Fig. 1 Conceptual map of the APRT calculation. Thick red curves indicate the trajectories in the PRD region in which the APRT was calculated.

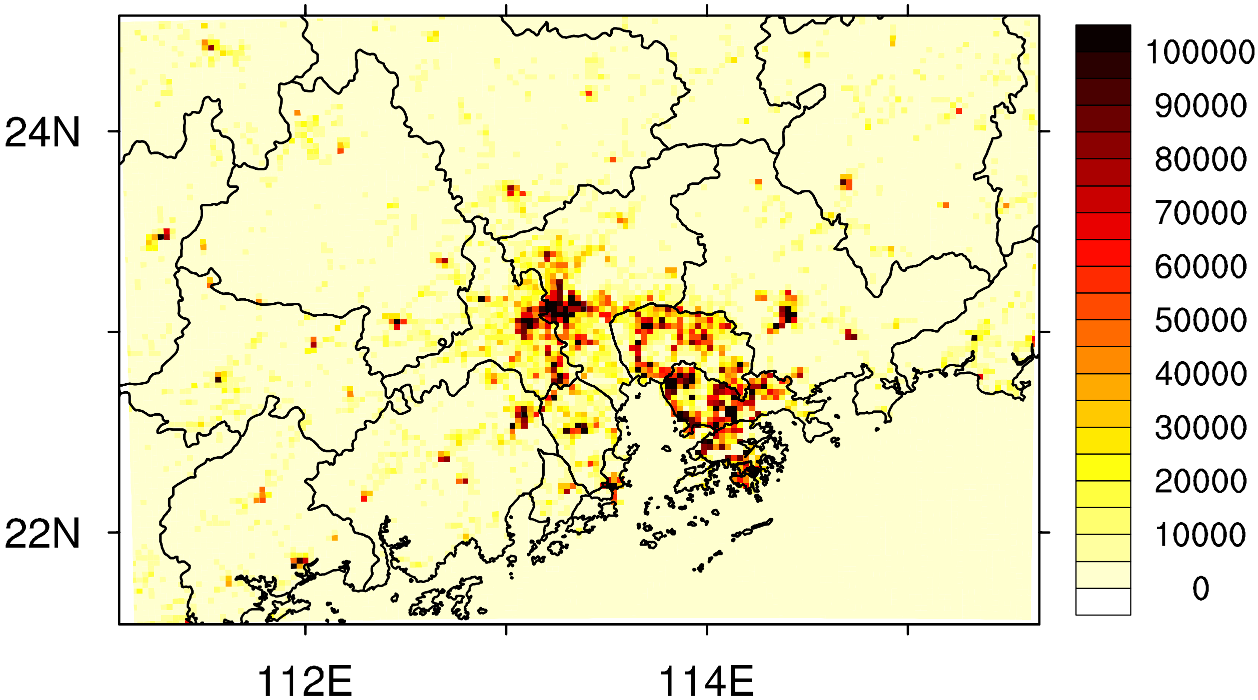

Fig. 2 Spatial distribution of the population density in 2014 at a resolution of 3 × 3 km^2.

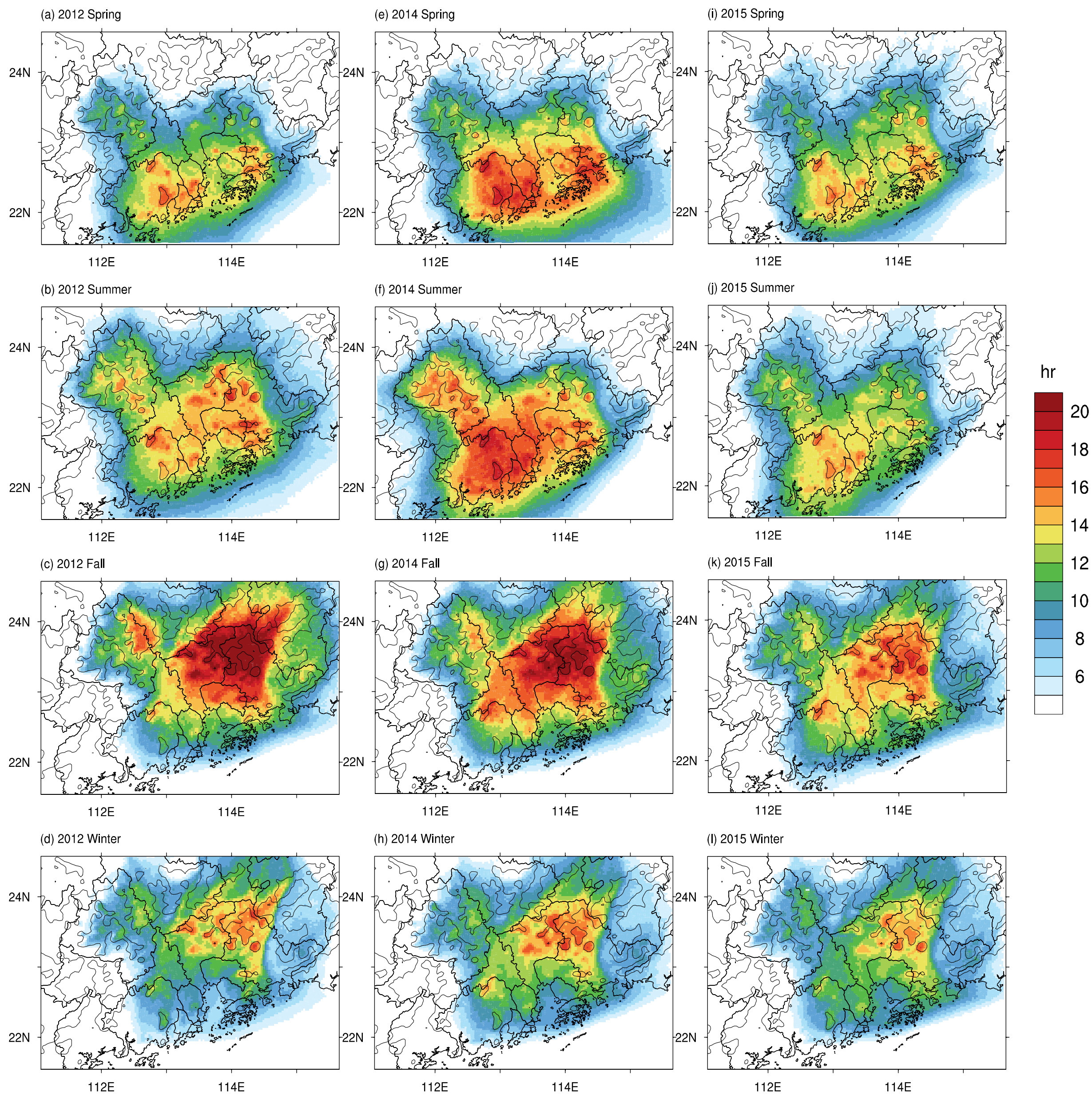

Fig. 3 The shading indicates the seasonal cycle of the APRT, and the grey contours indicate the topographic elevations of >200 m. (a)–(d) APRT from spring to winter in 2012; (e)–(h) APRT from spring to winter in 2014; (i)–(l) APRT from spring to winter in 2015.

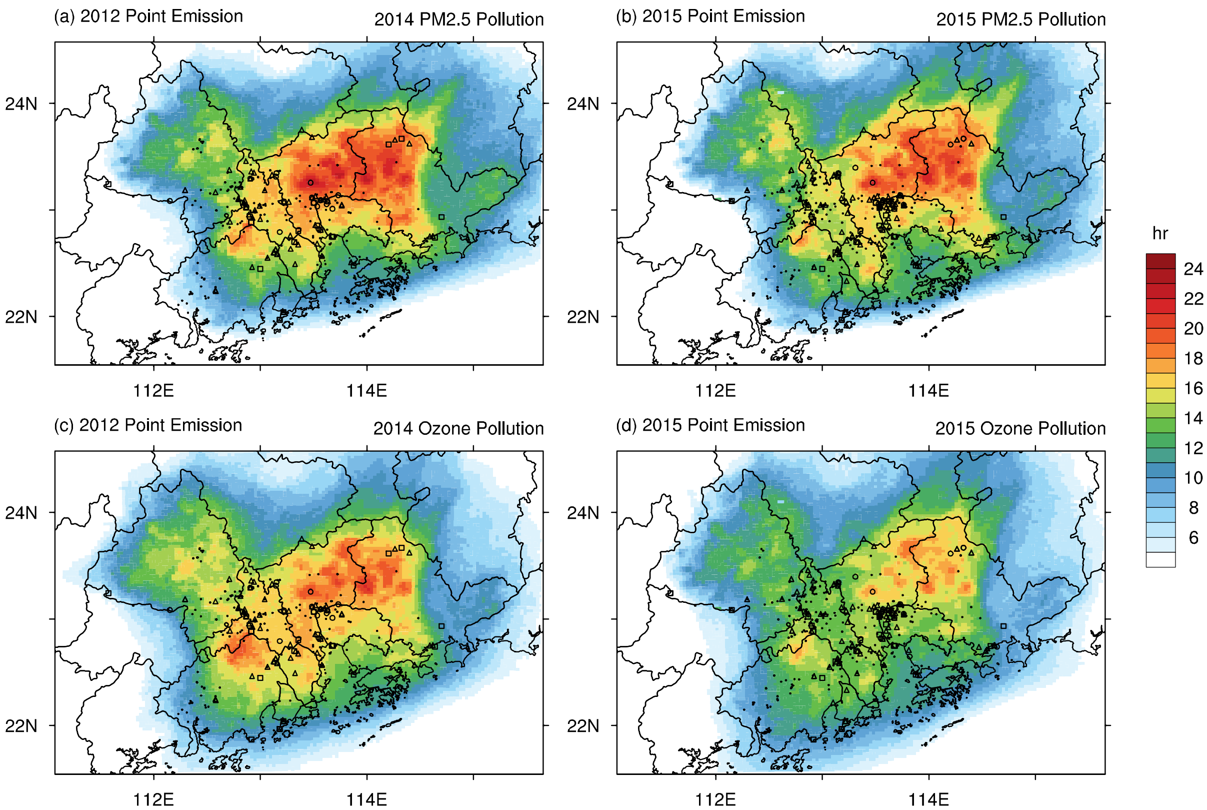

Fig. 4 Spatial distribution of the APRT on regional air pollution days with point emission data in the PRD region. (a) APRT in 2014 on $PM_{2.5}$ regional air pollution days with 2012 point emission distribution; (b) APRT in 2015 on $PM_{2.5}$ regional air pollution days with 2015 point emission distribution; (c) APRT in 2014 on O_3 regional air pollution days with 2012 point emission distribution; (d) APRT in 2015 on O_3 regional air pollution days with 2015 point emission distribution. Square represents SO_2, NO_x, or $PM_{2.5}$ emissions of >= 4000 short ton/year; circle represents emissions of >= 2000 short ton/year but <4000 short ton/year; triangle represents emissions >= 500 short ton/year but <2000 short ton/year; dot represents emissions >= 100 short ton/year but <500 short ton/year.

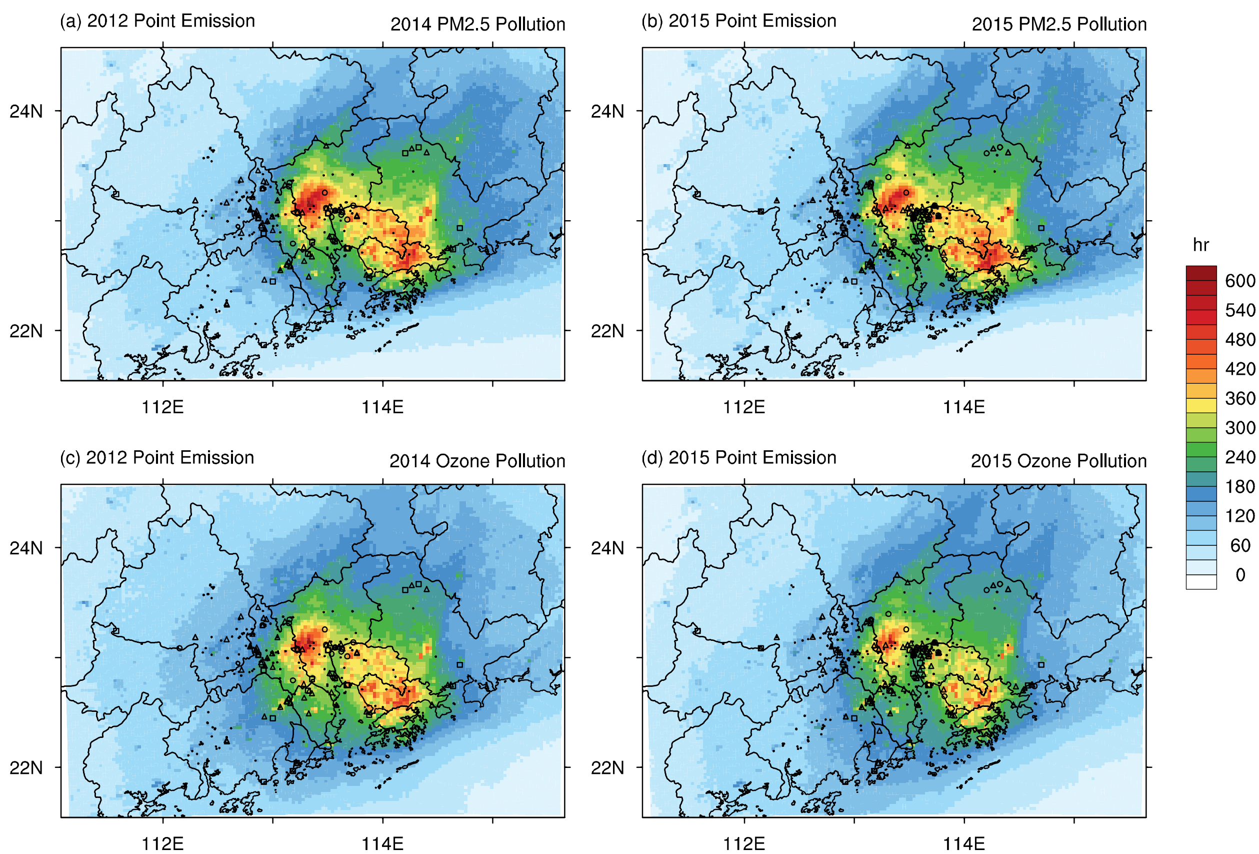

Fig. 5 Spatial distribution of PEAP in regional air pollution days with point emission data in the PRD region.

Table 1 Seasonal maximum APRT, seasonal mean APRT, $PM_{2.5}$ concentration, and O_3 concentration in 2012, 2014, and 2015

Seasons	Variables	2012	2014	2015
Spring	APRT_MAX (h)	17.0	19.2	16.3
	APRT_AVG (h)	9.3	10.1	8.9
	$PM_{2.5}$ (μg/m^3)	/	40.5	29.4
	O_3 (μg/m^3)	/	70.4	71.7
Summer	APRT_MAX (h)	18.2	20.0	16.4
	APRT_AVG (h)	9.6	10.7	9.4
	$PM_{2.5}$ (μg/m^3)	/	24.8	23.9
	O_3 (μg/m^3)	/	84.0	76.6
Fall	APRT_MAX (h)	24.1	22.4	19.2
	APRT_AVG (h)	11.3	11.0	9.8
	$PM_{2.5}$ (μg/m^3)	/	47.6	38.4
	O_3 (μg/m^3)	/	103.3	85.6
Winter	APRT_MAX (h)	17.4	17.9	17.0
	APRT_AVG (h)	8.9	9.2	9.0
	$PM_{2.5}$ (μg/m^3)	/	55	43.2
	O_3 (μg/m^3)	/	66.0	55.2

Figure
Click here to download Figure: Figure.pdf

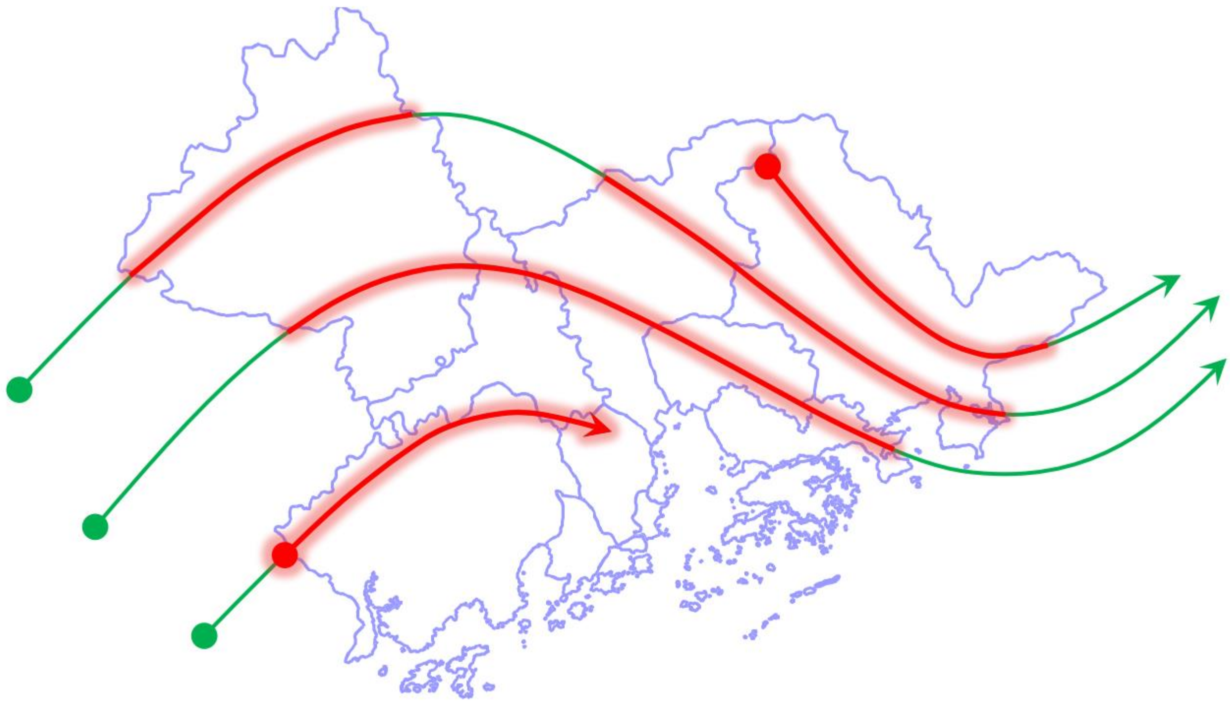

Fig. 1 Conceptual map of the APRT calculation. Thick red curves indicate the trajectories in the PRD region in which the APRT was calculated.

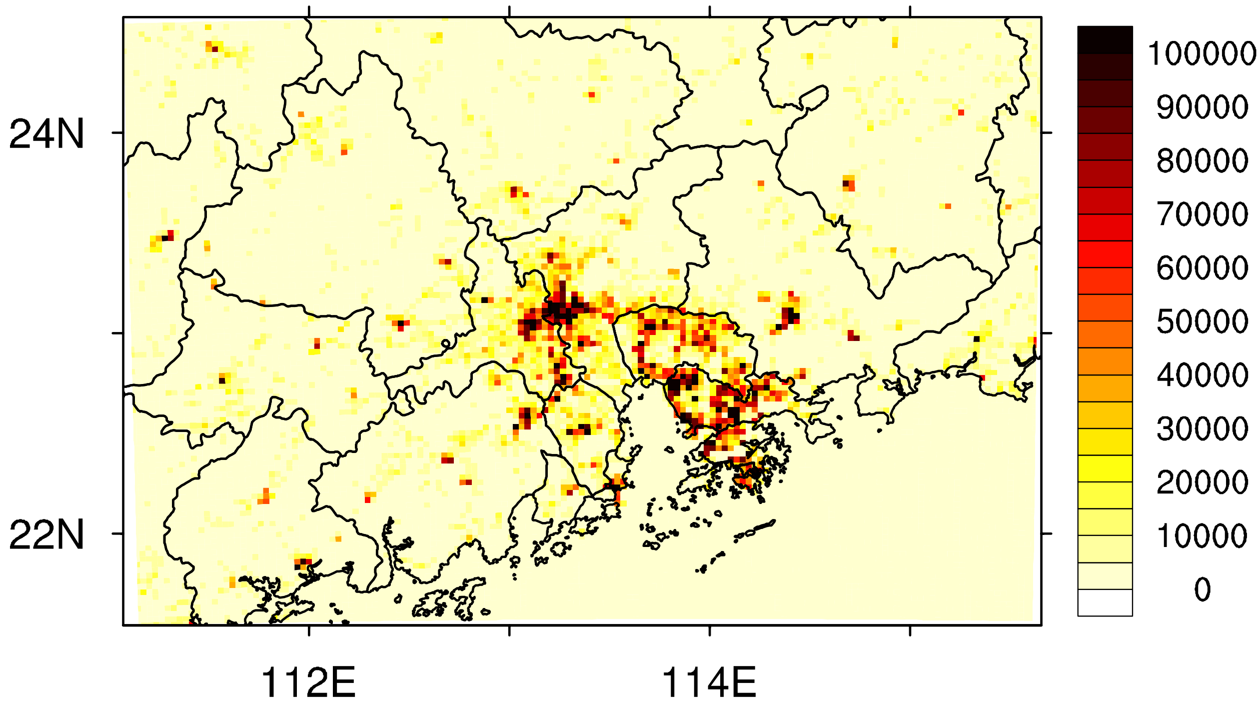

Fig. 2 Spatial distribution of the population density in 2014 at a resolution of 3 × 3 km^2.

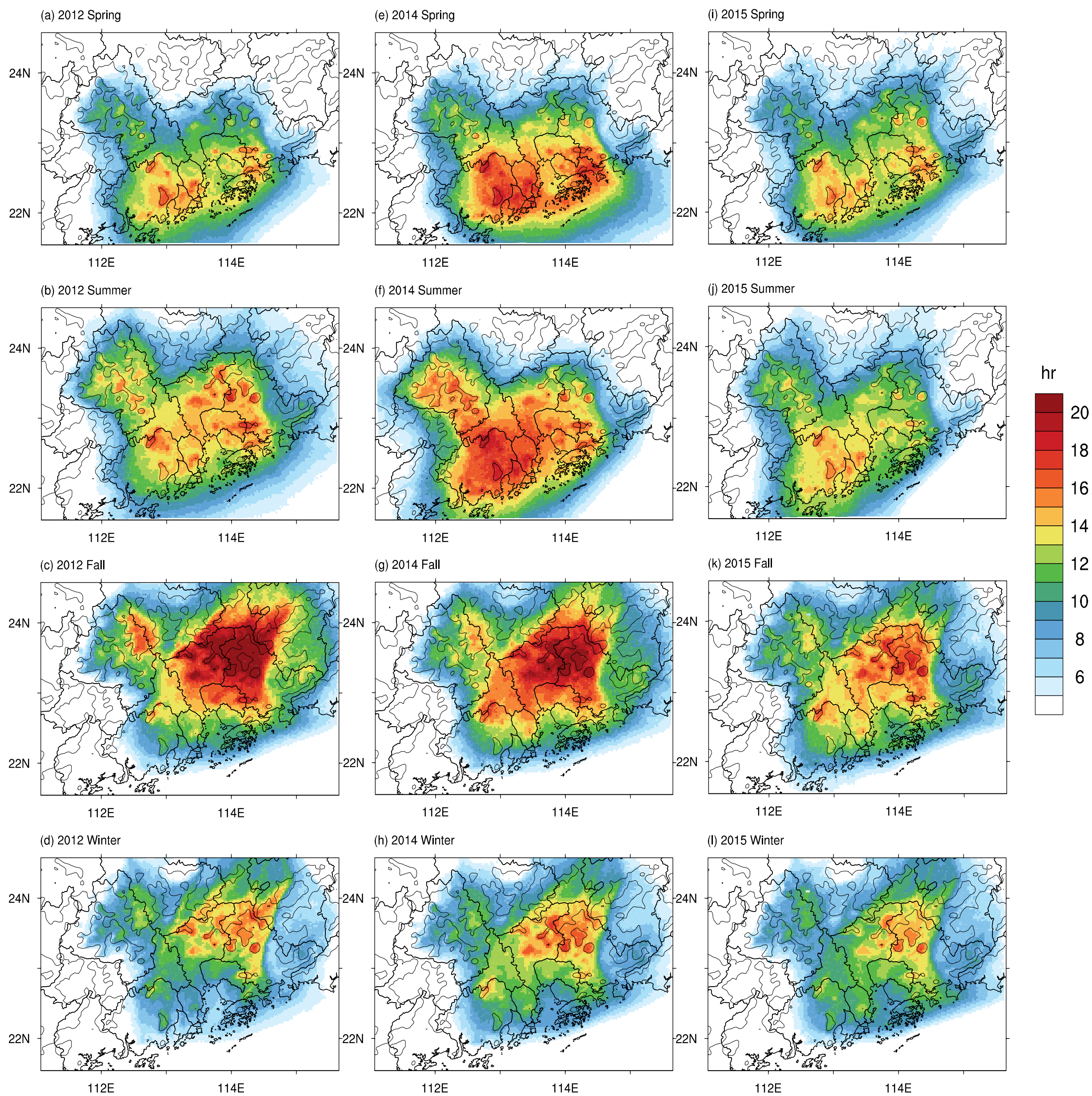

Fig. 3 The shading indicates the seasonal cycle of the APRT, and the grey contours indicate the topographic elevations of >200 m. (a)–(d) APRT from spring to winter in 2012; (e)–(h) APRT from spring to winter in 2014; (i)–(l) APRT from spring to winter in 2015.

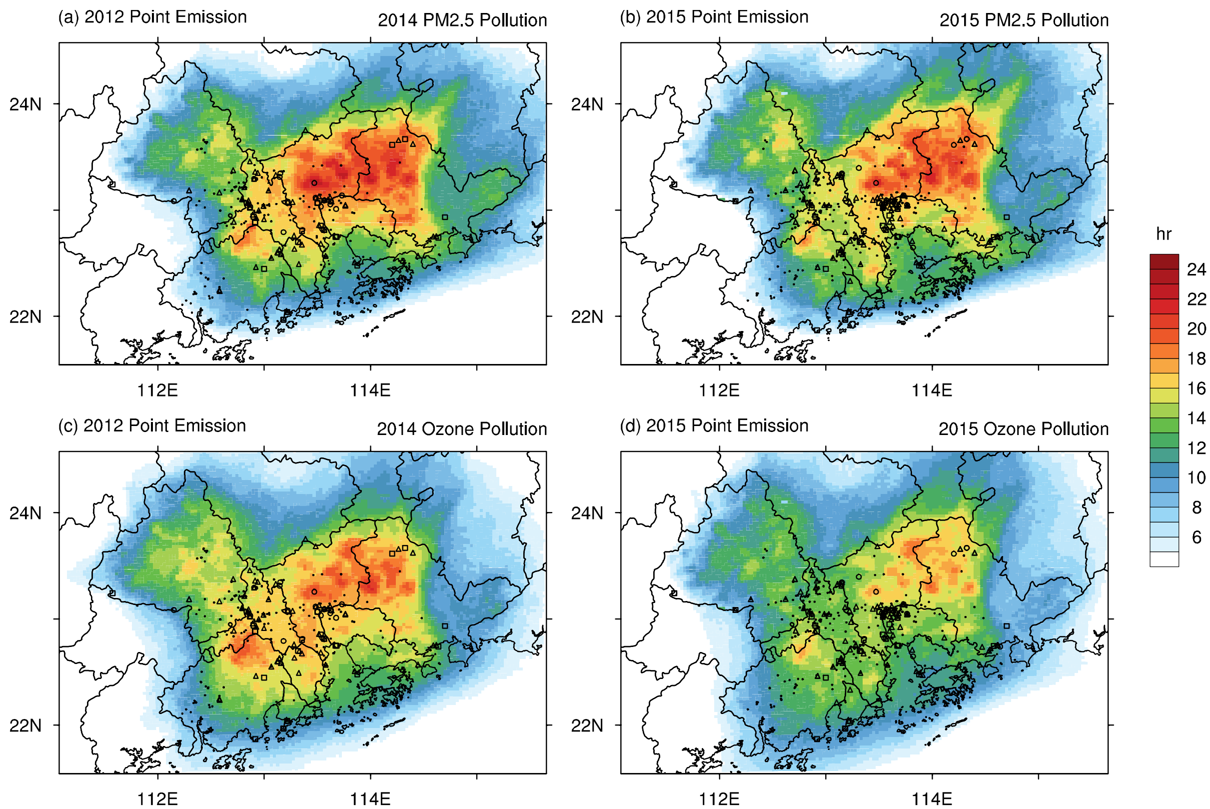

Fig. 4 Spatial distribution of the APRT on regional air pollution days with point emission data in the PRD region. (a) APRT in 2014 on $PM_{2.5}$ regional air pollution days with 2012 point emission distribution; (b) APRT in 2015 on $PM_{2.5}$ regional air pollution days with 2015 point emission distribution; (c) APRT in 2014 on O_3 regional air pollution days with 2012 point emission distribution; (d) APRT in 2015 on O_3 regional air pollution days with 2015 point emission distribution. Square represents SO_2, NO_x, or $PM_{2.5}$ emissions of >= 4000 short ton/year; circle represents emissions of >= 2000 short ton/year but <4000 short ton/year; triangle represents emissions >= 500 short ton/year but <2000 short ton/year; dot represents emissions >= 100 short ton/year but <500 short ton/year.

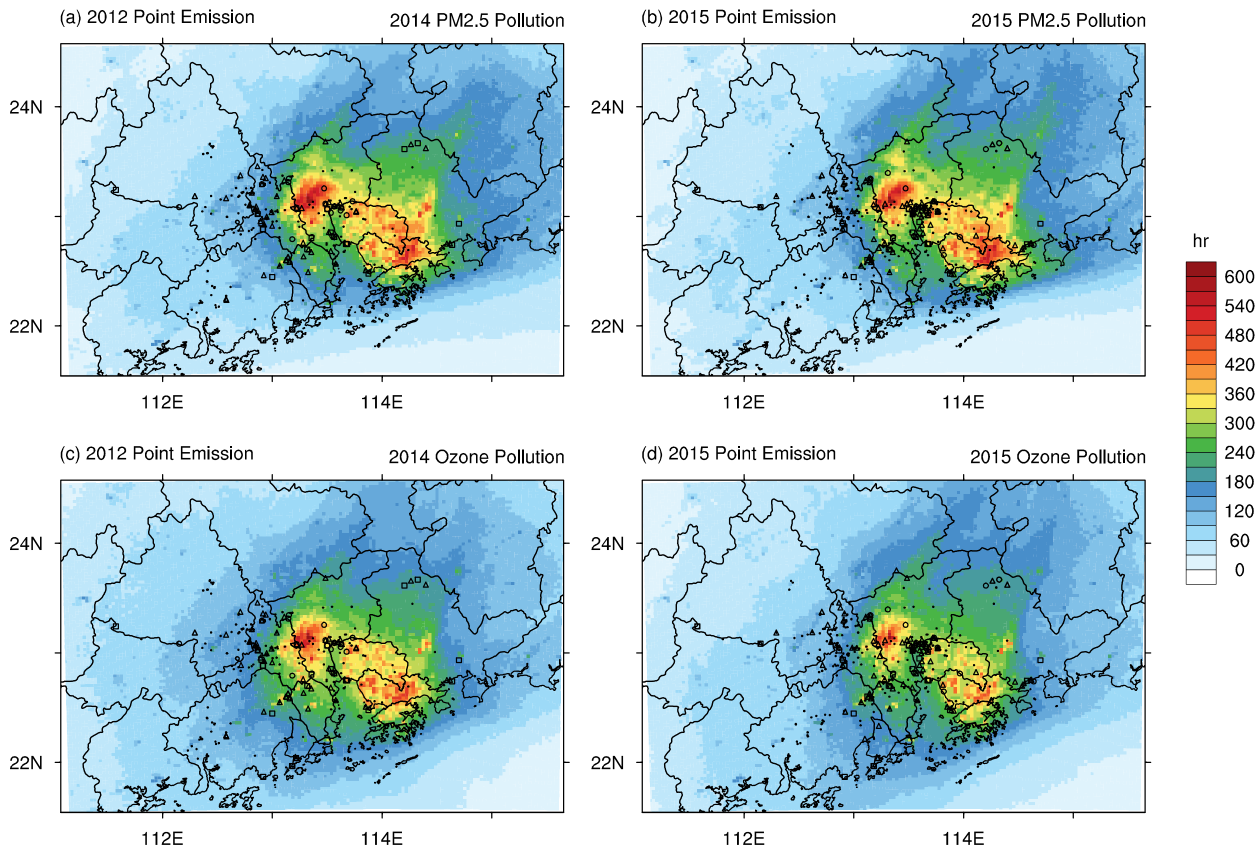

Fig. 5 Spatial distribution of PEAP in regional air pollution days with point emission data in the PRD region.